

Biomedical Paper

Optimization of Multiple-Isocenter Treatment Planning for Linac-Based Stereotactic Radiosurgery

Rui Liao, M.S.E., Jeffery A. Williams, M.D., Lee Myers, Ph.D., Shidon Li, Ph.D.,
Russell H. Taylor, Ph.D., and Christos Davatzikos, Ph.D.

Departments of Radiology (R.L., R.H.T., C.D.), Neurosurgery (J.A.W., L.M.), and Radiation Oncology (S.L.), School of Medicine, Departments of Biomedical Engineering (R.L.) and Computer Science (R.H.T., C.D.), School of Engineering, and Center for Computer Integrated Surgical Systems and Technology (R.H.T., C.D.), Johns Hopkins University, Baltimore, Maryland

ABSTRACT Objective: Computer-assisted treatment planning for linac-based radiosurgery is still an open research problem, especially for multiple-isocenter procedures, primarily due to its high complexity and computational requirements. This paper focuses on the optimization of multiple-isocenter treatment planning for linac systems, and addresses several important issues associated with multiple isocenters, such as dose conformality, homogeneity, and optimization of isocenter position and dose.

Methods: The key idea behind our approach is that the desired dose distribution can be decomposed into a number of fundamental components. In the current paper, an analytical form, the so-called Ellipsoidal Dose Distribution Estimation (EDDE) model, represents each component. We establish ways (arc configurations) to achieve such ellipsoidal doses of arbitrary position, orientation, and size. Since the EDDE model is described by relatively few parameters, it allows very quick estimation of the dose distribution corresponding to a particular isocenter and thus makes the optimization of isocenter position very efficient. It is further used in a framework for optimal treatment planning, in which a number of ellipsoidal dose distributions, each corresponding to a different isocenter, are optimally placed to cover the target while sparing healthy tissue.

Results: The general ellipsoidal dose distribution of linac-based radiosurgery is summarized as a mathematical model with the aid of supporting experiments. Comparisons between the EDDE-optimized and clinically implemented plans are made, revealing the superior performance of the former. In addition, a dramatic reduction in planning time is achieved using the EDDE model.

Conclusion: The proposed EDDE model is a useful and effective dose model in multiple-isocenter treatment planning for linac-based radiosurgery. *Comp Aid Surg* 5:220–233 (2000). ©2000 Wiley-Liss, Inc.

Key words: radiosurgery, linac, plan optimization, inverse treatment planning, multiple-isocenter treatment

INTRODUCTION

Since the introduction of stereotactic radiosurgery based upon the linear accelerator (linac) in the

1980's,^{8,14,24,32} optimization of the dose distribution (in order to deliver a high, uniform dose to the

Address correspondence/reprint requests to: Christos Davatzikos, Ph.D., Department of Radiology, JHOC 3230, Johns Hopkins University School of Medicine, 601 N. Caroline St., Baltimore, MD 21287; E-mail: hristos@rad.jhu.edu.

target volume while minimizing the dose to surrounding normal structures) has been actively pursued. Initial linac radiosurgery was standard and relatively simple. Several non-coplanar arcs were converged to a point (the isocenter) by rotating the gantry at fixed table angles. Cylindrical collimators with different diameters were used to conform to the different sizes of the targets. Many modified linac systems have since been developed^{4,9,11,13,17,21,30} to improve the optimization of radiosurgery. Elliptical collimators^{23,25} and dynamic field shaping^{12,19} have also been investigated, while the miniature multileaf collimator (MMLC) has attracted considerable attention for development of optimization.^{10,26} Since linac systems are still the most widely available devices for radiosurgery in most clinical centers, and because the potential of the current linac systems has not been fully developed, we have concentrated upon improving the optimization of dose delivery via modified linac systems.

In general, the dose distribution produced by a single isocenter treatment is nearly spherical and homogeneous around the isocenter for both linac systems⁹ and gamma-knife units.²⁰ In order to treat non-spherical, irregular, or large tumors that cannot be covered by the largest available collimator, multiple-isocenter plans are necessary. While dose conformality is improved, the inhomogeneity within the target is also increased by using multiple isocenters. Although an accurate biological effect model of the normal tissue and tumor corresponding to a single-fraction high dose has still not been established, it is believed that dose homogeneity reduces complication rates.¹⁸ Accordingly, we seek optimal conformality to the target²⁸ and minimum-dose inhomogeneity within the target. Many previously reported linac systems were, however, based upon a single isocenter, i.e., they did not take into account the important issues that arise from the use of multiple isocenters. Most of the work on multiple isocenters has been based on the gamma-knife,^{2,6} but as multiple-isocenter plans are commonly used in linac systems, we focus our attention on them in this paper.

The most important issue for the development of multiple-isocenter plans is the optimization of the parameters for the isocenters, including the positions of the isocenters, the size of the collimator at the isocenter (referred to as *isocenter size*), and the dose prescribed at the isocenter (*isocenter dose*). Suboptimal selection of these parameters can result in highly inhomogeneous dose distributions, including hot spots and under-irradiated areas. Thus, some groups have developed tables showing

the optimal spacing of isocenters having disparate diameters and combinations,¹⁷ and these may be used to guide isocenter placement.

Despite the significance of the optimization of isocenter parameters, many reported treatment planning systems^{9,17} still require a trial-and-error procedure for placement of the isocenters, which can inevitably result in a sub-optimal plan. Other systems^{11,33} have incorporated isocenter position and collimator size as optimization parameters. These methods require a great deal of computation time if no method for fast dose calculation is employed. For instance, in the report by Yan et al.³³ only the dose on the surface of the target was optimized, instead of the dose in the target volume, in order to reduce the computational demands. For this method, the homogeneity of the dose within the treatment volume was not considered. In addition, the large number of parameters for that method could make the optimization problem susceptible to local minima.

In order to reduce the computational requirements for dosimetry, investigators have considered fast dose models based on modeling the dose distribution resulting from a collection of beams, rather than considering the contribution of each beam individually. A dose calculation model based on the mini-arc has been studied¹ in which a beam arc was divided into 20-degree segments (mini-arcs), and the dose model of a 20-degree mini-arc was pre-calculated and stored as look-up tables. Later, a spherical dose model was reported²⁷ which used an analytical form to model the spherical dose distribution for an isocenter having equally placed beam arcs. In order to overcome the limitations of spherical dose models that arise when targets of complex shape are treated, other investigators have proposed ellipsoidal dose models.^{15,22}

Approaches based on dose models expedite the dose calculation procedure tremendously, and therefore make it possible to include isocenter parameters (such as position and size) in the plan optimization while maintaining a reasonable computational load. Although many groups have summarized their experience with producing ellipsoidal dose distributions, none of these methods was formulated within a mathematical framework. The formulation and experimental verification of an ellipsoidal dose distribution model is the primary contribution of this paper.

The key idea behind our approach is that the desired dose distribution can be decomposed into a number of fundamental components. In the current paper, each component is given by an analytical form, the so-called *Ellipsoidal Dose Distribution*

Estimation (EDDE) model. We establish ways (arc configurations) to achieve such ellipsoidal doses of arbitrary position, orientation, and size. Since an ellipsoidal dose model is comprised of relatively few parameters, it allows the use of dosimetry in plan optimization, especially isocenter position, in a computationally very efficient way. Most importantly, it allows us to incorporate the position and prescribed dose for each isocenter, in addition to other parameters, into the multiple-isocenter optimization scheme. Experiments using clinical cases are described to illustrate the advantages and limitations of our method. Having established the EDDE model, we then use it in an optimization framework for treatment planning.

MATERIALS AND METHODS

Overview

Our experiments have indicated that the dose distribution around one isocenter can be approximated by a set of ellipsoids, each of which corresponds to one isodose surface. Our experience agrees with experiments by other investigators.^{15,17,21,22} We use this fact in order to derive a mathematical description of the dose distribution, the EDDE model, in which a *reference ellipsoid*, corresponding to 80% isodose, is first defined. According to the reference ellipsoid and to a model for the dose fall-off as a function of distance from the isocenter, the actual dose contributed by one isocenter can be estimated for each point in the area of interest that includes one or more organs of interest and the target. Having established this dose model, we then use it to find an optimal plan. This is done by covering the target with a number of ellipsoidal components, each of which contributes to the total dose according to the EDDE model. This optimization procedure consists of the following steps:

Step 1: Optimal placement of a number of reference ellipsoids, one corresponding to each isocenter (Fig. 1), so that optimal coverage of the target is achieved while critical structures are spared.

Step 2: Determination of a number of *subarcs*, i.e., parts of a full arc that can be traversed by the linac system, for each isocenter. These subarcs are placed so that they can produce the ellipsoidal dose distribution defined by the reference ellipsoid.

Step 3: Optimization of the weighting of each subarc, using the primary dose model.¹⁶ The optimization criterion is the discrepancy between the actual dose distribution and the dose

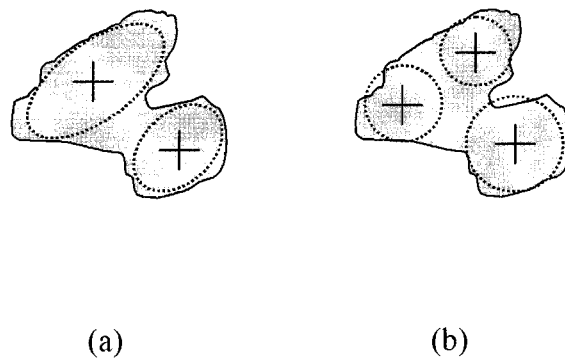


Fig. 1. An irregularly shaped target treated by multiple isocenters, shown in a 2D slice. (A) Using two reference ellipsoids; (B) A plan using three isocenters.

distribution predicted by our model in the first step.

These steps are described in the *Optimization Procedures* section. In particular, Step 1 is described under *Ellipsoid placement*. Steps 2 and 3 are described under *Arc selection and dose optimization*. However, before describing the optimal placement of the ellipsoidal models, we first derive the EDDE model and the formulae that approximate the dose distribution as a function of distance from the center of each ellipsoid.

Data Acquisition and Treatment Planning Systems

Our treatment planning is designed for use with a modified 10-MeV linear accelerator in the Brain Tumor Radiosurgery Center at Johns Hopkins Hospital, in which a circular collimator and a fixed dose weighting is used for one beam subarc. The available collimator sizes are currently 13, 16, 18, 21, 28, and 34 mm. Brain images are acquired with a Picker CT Scanner,³¹ and have dimensions of 512×512 pixels per slice and a resolution of 0.938×0.938 mm per pixel in the X and Y directions. The slice thickness is typically 2.0 mm. The target volume is delineated manually. Critical structures can be defined either manually, based on the patient's images, or via elastic adaptation of anatomical atlases to the patient's scans.⁵ Stereotactic coordinates are obtained via the Brown-Roberts-Wells (BRW) stereotactic frame for both CT scanning and treatment planning. We compare our results against the semi-manual plans generated routinely in the clinic via the BrainLab system (BrainLab Inc., Palo Alto, CA).

Ellipsoidal Dose Distribution Estimation (EDDE) Model

In the EDDE model, the dose distribution corresponding to a single isocenter is modeled by a reference ellipsoid and a dose fall-off function. This dose model serves as a building block in our method and is described in this section. In order to establish the EDDE model, we addressed three issues. We first examined how to determine a configuration of subarcs, especially in terms of their position and weighting, that can produce a particular ellipsoidal dose distribution. Second, we derived an analytical model for different isodose surfaces corresponding to a reference ellipsoid. We found that these isodose surfaces can also be well approximated by ellipsoids, up to a certain isodose level, and we experimentally determined an analytical form for the dose fall-off. Finally, we designed simulated experiments to demonstrate that our ellipsoidal dose model is independent of the position, orientation, and size of the target (within a normalization factor). The position, orientation, and size invariance is a fundamental issue when using a dose model, since it allows us to use the same model for any target. This issue is clarified by experimental results presented in the Results section of this paper.

In order to derive and test the EDDE model, we used the hemispherical head phantom^{15,27} as the volume of interest, and placed an ellipsoid inside as the target. We then derived the subarc configuration and weighting for this ellipsoidal target, and calculated the resultant dose distribution. The various isodose surfaces were modeled as ellipsoids whose spacing was determined experimentally by fitting a parametric dose fall-off function to the calculated dose distribution. Details for each step were as follows.

Reference ellipsoid

A reference ellipsoid is defined as follows:

$$\frac{x^2}{a^2} + \frac{y^2}{a^2} + \frac{z^2}{b^2} = 1, \quad (b \geq a) \quad (1)$$

The coordinates (x, y, z) used here are transformed to the ellipsoid's frame, i.e., the three axes of the ellipsoid define the $X, Y,$ and Z axes. We therefore describe arbitrarily shaped and oriented ellipsoids in this formula. We have made the two major axes of the reference ellipsoid equal in length because we only have circular collimators in our current system. Therefore, we could only compare our results with the clinical plans if we restricted this

parameter. If elliptical collimators are available,²⁵ the three axes could become independent without loss of generality. Moreover, it will be shown later that the ellipsoidal dose distribution can actually be achieved even by circular collimators.

Subarc configuration

The subarc configuration that produces a given reference ellipsoid is found by placing the isocenter at the center of the ellipsoid, then selecting the collimator size according to the beam's-eye view (BEV) of the reference ellipsoid. We first project the ellipsoid to the available arc space (In our system, the table angle ranges from 0 to 180 degrees, and the gantry angle ranges from 0 to 135 degrees due to physical constraints). This results in an elliptical profile for each orientation. Since, in this paper, we assume that only circular collimators are available, we define the smallest circle that encompasses the elliptical profile as the *proper collimator size* at each orientation. The proper collimator size is, in general, different at different orientations, since it depends on the BEV of the ellipsoid. However, the linac system is based on a continuous sweep of an arc or subarc, using the same collimator size for the whole sweep. Moreover, the available collimator sizes are limited. Therefore, we choose to place subarcs where the proper collimator sizes are available. Since the collimator size is locked along each subarc, we choose to place subarcs in areas where the proper collimator size varies relatively slowly with gantry angle. Following this procedure, we generate an *arc map* for all available subarcs (e.g., Figure 2). The nearest available collimator size is selected for a particular subarc. The length of the subarc is defined so that all proper collimator sizes for the orientation of the subarc are within 1 mm of the subarc's collimator size. A surgeon can then select several arcs (usually 5 to 10) from the arc map based on the following two rules. First, the subarcs with the smallest collimator size (e.g., the two 16-mm subarcs in Figure 2) which correspond to the long axis of the reference ellipsoid are selected, because we want the dose distribution to be maintained in that direction. Second, some space is allowed between subarcs and overlap of subarcs between multiple isocenters is avoided, because an evenly shaped dose distribution is desired. Automation of this procedure has not been implemented at this point.

Dose calculation for a reference ellipsoid

Having determined the subarc configuration for each reference ellipsoid, we next determine the

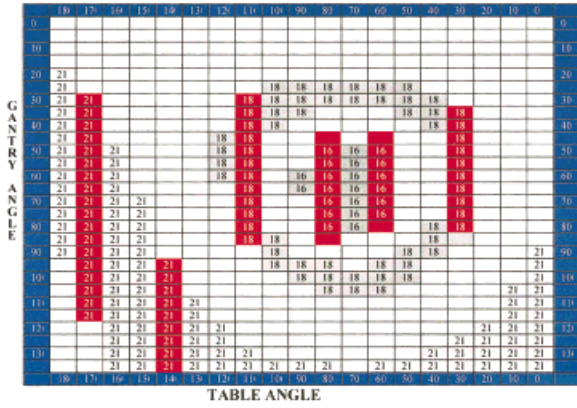


Fig. 2. The arc map for a reference ellipsoid with long axis $Z = 21$ mm and short axis $X = Y = 16$ mm, rotated by $(\theta_x = 30^\circ, \theta_y = 10^\circ, \theta_z = 50^\circ)$. Abscissa is table angle; ordinate is gantry angle. Each box is filled with the proper collimator size for the corresponding angle, which is determined from the beam's-eye view of the reference ellipsoid, as described in the text. Unfilled boxes imply that that particular collimator size is not available, and hence that angle cannot be used. Of the unfilled boxes, the gray ones correspond to proper collimator sizes that are less than 1 mm different from available ones. All vertical gray lines correspond to a subarc (partial sweep of the linac). Dark lines are selected arcs, which produce an ellipsoidal dose distribution.

beam weighting for each subarc, so that the desired ellipsoidal dose distribution is achieved. Let $W_i, i \in \{1, \dots, M\}$, be the weights of M subarcs irradiating the target ellipsoid, and $W = [W_1, W_2, \dots, W_M]^T$, be the vector of weights to be optimized. If $b_i(x, y, z) = b_i(v)$ is a function reflecting the dose delivered by the i -th subarc to each point v , the total dose at that point is given by the function

$$D(W, v) = \sum_{i=1}^M W_i b_i(v) \quad (2)$$

Since the dose distribution is linear to the beam weighting, we simply use the least-square-error method to minimize the cost function:

$$C(W) = \sum_{v_m \in \text{brain}} [D(W, v_m) - T(v_m)]^2, T(v_m) = \begin{cases} 1, & v_m \in \text{target} \\ 0, & v_m \in \text{normal} \end{cases} \quad (3)$$

where $D(W, v_m)$ is the dose received by the point v_m , and $T(v_m)$ is the desired dose to that point. The dose is normalized to one at the isocenter. We

calculate the dose distribution using the single-beam model.¹⁶

Isodose ellipsoids and dose fall-off model

Following the steps described above, we generate an ellipsoidal dose distribution which covers the target (reference ellipsoid) at the 80% isodose level. We have determined that any other isodose surface can be approximated by another ellipsoid of the following form:

$$\frac{x^2}{a^2} + \frac{y^2}{a^2} + \frac{z^2}{s \cdot b^2} = RD^2, \quad (b > a) \quad (4)$$

This is referred to as an *isodose ellipsoid*, in which RD is related to the isodose level of the ellipsoid, or equivalently the distance of the isodose ellipsoid from the center of the reference ellipsoid. We introduced the factor s because we found that the isodose surfaces tend to become increasingly elongated with distance from the reference ellipsoid in the long axis direction. Experimentally, we determined that $s = b/a$ can be used to match the isodose ellipsoids to the isodose surface very well.

Because of the way we defined the isodose ellipsoids, the isodose surfaces are described by one parameter RD , i.e., each value of RD corresponds to a different isodose surface. The next step is to find the relationship between RD and isodose levels, which will yield a mathematical description of the dose distribution. In order to find this relationship, we used a non-linear least-squares curve fitting technique and experimental dosimetry data. After examining several possible functions, we found that the relationship between isodose level and radial distance can be described by a modified Cathy function,

$$D = f(RD) = \frac{\Delta^{2\beta}}{(|RD|^\alpha + \Delta^2)^\beta} \quad (5)$$

where D is the isodose level, normalized to 1, $\Delta = 1.1152$, $\alpha = 6.7688$, and $\beta = 0.3370$. Figure 3 shows the fit of this curve to data points.

These procedures yield a very simple form of the dose model. Specifically, in order to calculate the dose distribution of one isocenter with several arcs, it is only necessary to calculate the Mahalanobis distance, RD , from any point to the isocenter, instead of calculating the distance and depth from that point to hundreds of beams. In other words, given a reference ellipsoid with the form of Equation 1, we compute RD from Equation 4 for each point in the tissue, then the dose contributed

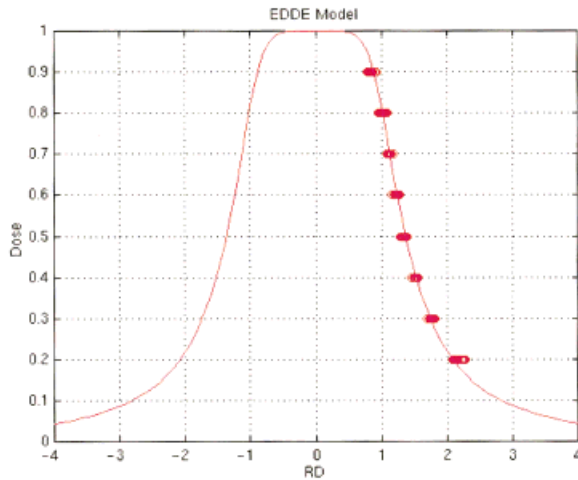


Fig. 3. Fit of a parametric function to data points showing the dose fall-off for the EDDE Model. Data points are shown for all collimator size combinations available in our treatment center. The curve is extended symmetrically for better visualization. Note that the modified Cathy curve fits the data very precisely, regardless of the collimator size. This is very important and it enables us to construct the EDDE model, which is independent of the target size.

by this isocenter is given by Equation 5. This model could reduce the calculation time by a factor of more than 100. Because this model is just a simplified approximation of the dose distribution, we call it an estimation model.

Optimization Procedures

There are two major difficulties that arise in multiple-isocenter treatment planning:

- 1) *Isocenter placement.* In general, isocenters must be placed according to the shape of the target. However, the manual placement of several isocenters is a difficult task, since a surgeon has to mentally reconstruct the complex three-dimensional shape of a target, and its position relative to surrounding structures, from cross-sectional images.
- 2) *Target partitioning.* For a single isocenter plan, the collimator size is usually selected based on the BEV. However, in multiple-isocenter cases, effectively only part of the tumor is covered by a single isocenter. The partitioning of the tumor, and therefore the corresponding BEV of each partition, is not known in advance if this partitioning is part of the optimization procedure.

By introducing the EDDE model, these two important issues are addressed simultaneously. In

particular, the target is partitioned using sets of ellipsoidal surfaces. The shapes and locations of these ellipsoids are calculated simultaneously by our optimization method. Moreover, for each ellipsoid, the arc configuration is directly derived from the procedure discussed in the *Subarc configuration* section. Consequently, target partitioning and subarc configuration are derived from a very fast optimization algorithm. Figure 4 shows an example of an ellipsoid placement using the procedures described in the following sections. In addition, our method is a quantitative methodology, since we have a model for deriving the dose distribution from the reference ellipsoid (see Equations 4 and 5).

In the previous section we described how we produce an arbitrarily orientated ellipsoidal dose distribution around a single isocenter, using the EDDE model. In this section, we describe how we place a number of reference ellipsoids so that they maximally cover a given target while causing minimal damage to critical structures. Based on our dose model, the whole treatment planning procedure consists of three steps: ellipsoid placement (isocenter optimization), subarc configuration, and beam weighting optimization. Since subarc configuration is part of the EDDE model and has been described previously, we now concentrate on the remaining steps.

Tissue dose response model

Before we can discuss the isocenter optimization, we need to define a model describing how a certain

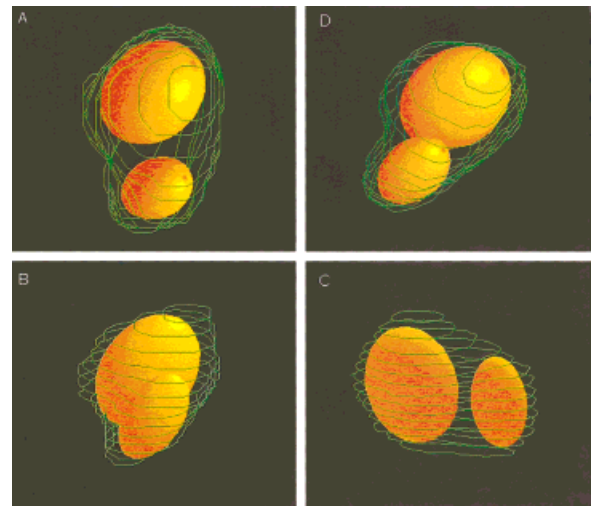


Fig. 4. 3D views of ellipsoid placement using the EDDE model overlaid on the target contours. Two reference ellipsoids are placed. (A) axial view; (B) coronal view; (C) sagittal view; (D) arbitrary orientation.

type of tissue responds to a certain dose of irradiation. Since currently there is no consensus on which is the correct radiobiological model, we simply use the quadratic function. The modular design of our algorithm makes it easy to replace this function by any other function. For planning convenience, we define lower and upper dose bounds for each type of tissue concerned. Then, the penalty function for each point is

$$q(D) = \begin{cases} \delta_h(D - T_h)^2, & \text{for } (D > T_h) \\ \delta_l(D - T_l)^2, & \text{for } (D < T_l) \end{cases} \quad (6)$$

in which D is the dose delivered to the point, T_h and T_l are upper and lower dose bounds, respectively, δ_h and δ_l are corresponding *importance factors*. Typically, both upper and lower dose bounds are used for the target; for critical structures and normal tissue, only the upper dose bound is used (since $\delta_l = 0$).

In an ideal world, the exact position of each critical structure is known exactly. However, in a realistic setup there are various sources of error which might contribute to the lack of certainty regarding the exact structure location. For example, there are registration errors between physical (patient) and image coordinates. Moreover, structures might be defined via anatomical atlases,⁵ which can be adapted to the patient's individual anatomy with only limited accuracy. Even with perfect registration, brain anatomy does not exactly define brain function, because of inter-individual functional variability. Finally, even manual definition of functionally critical regions is well known to be prone to errors and inter-rater variability. In order to account for such position uncertainties, we assume that we know the type of structure present at each location in the brain with only a certain degree of probability. In particular, if each point belongs to one of K types of structures with probability p_i , $i \in \{1, \dots, K\}$, then the total penalty corresponding to one point is

$$Q(D) = \sum_{i=1}^K p_i q_i(D) \quad (7)$$

where $q_i(D)$ is from Equation 6, for each type of tissue.

Ellipsoid placement

For each reference ellipsoid, there are 9 parameters: the isocenter location (X, Y, Z), the isocenter dose (DI), the axes lengths (a, b), and the rotation angles

($\theta_x, \theta_y, \theta_z$) measured with respect to the three coordinate axes of the patient's images. Let $E_i = [X, Y, Z, a, b, \theta_x, \theta_y, \theta_z, DI]^T$, $i \in \{1, \dots, N\}$, be the parameter vector of the i -th reference ellipsoid, then the set of parameters to be optimized is $E = [E_1, E_2, \dots, E_N]^T$, for N reference ellipsoids. In order to optimize the placement of these ellipsoids, we calculate the dose distribution through these reference ellipsoids by adding their contribution together, and then use certain dose optimization criteria to optimize the dose distribution. The dose distribution for a configuration with N isocenters is calculated by

$$D(x, y, z) = D(v) = \sum_{i=1}^N DI_i f(RD_i) \quad (8)$$

where DI_i is the isocenter dose, initially assigned as 1.0 to each isocenter, and $f(RD_i)$ is computed through Equation 5. The cost function we defined as an optimization criterion is

$$C(E) = \sum_j Q\{D(v_j)\} \quad (9)$$

This is the sum of the penalties applied to all sample points, in which $Q(D(v_j))$ is from the tissue dose response model above. Then we use Powell's method³³ to optimize the ellipsoid parameters E in terms of minimizing the cost function, Equation 9. Powell's method is suitable for this problem because it does not require the derivative of the cost function, and it converges to the result very fast. Since we only have limited collimator sizes, a and b are discrete variables. We have modified Powell's method to be able to optimize discrete parameters.

In order to initialize Powell's iterative optimization procedure, we use a heuristic algorithm that partitions the target into N regions, using a "cluster analysis" method, initially reported in Reference 3. This method is an iterative algorithm with the following steps:

Step 1: Place the first isocenter on the center of mass of the target. If more than one isocenter is requested, then go to Step 2; otherwise, terminate.

Step 2: Place an additional isocenter on the most distant point from the existing isocenter(s).

Step 3: Assign each point in the target to its nearest isocenter.

Step 4: Reposition the isocenters so that they coincide with the center of mass of the target

points assigned to them. If their position doesn't change significantly, go to Step 5; otherwise, go to Step 3.

Step 5: If more isocenters are to be added, repeat the iterative procedure above by sequentially adding one isocenter at a time; otherwise, stop.

As was mentioned earlier, the number of isocenters is predefined, but when this procedure terminates, the target is divided into a number of partitions equal to the number of isocenters. The initial guess of the reference ellipsoid is then the biggest sphere that is fully contained within the corresponding partition of the target.

The number of isocenters is not determined by our optimization algorithm, but is predefined by the physician. Since our algorithm does not require excessive computational time, it is practically feasible to compute the optimal plans for different numbers of isocenters and then select the minimum number of isocenters that results in an acceptable dose distribution. Our experiments have shown that, as intuitively expected, increasing the number of isocenters can improve conformality to the target. Therefore, practical considerations and time constraints limit the number of isocenters used. Moreover, it is possible to generate optimal plans for increasingly higher numbers of isocenters and stop at the number for which the dose conformality levels off, with only minor further improvement.

Arc selection and dose optimization

During the ellipsoid placement step in the previous section, we minimized the total dose within a number of structures that are considered critical and maximized the dose conformality and homogeneity to the target, according to the EDDE model. Following the subarc selection technique described in the *Subarc Configuration* section, we can readily determine the collimator size and orientation of each subarc, which yields the subarc configuration necessary to produce the optimal ellipsoids. In this section, we describe how we determine the weighting of each of the selected subarcs.

The EDDE model is only an approximation of the true dose distribution, being used to place a number of reference ellipsoids and determine the corresponding subarc configuration in a computationally efficient manner. However, when determining the weighting of each subarc, we use the thin beam dose model.¹⁶ In particular, dose calculation is performed using Equation 2, where the function $b(\cdot)$ is the cumulative dose delivered by a number of beams constituting a subarc; the contribution of each beam is given by the thin beam

model.¹⁶ Our goal is to minimize the difference between the dose distribution estimated by the EDDE model and that calculated by the single-beam dose model. This is because the former was the one used to optimally place a number of ellipsoids. We define the cost function as:

$$C(W) = \sum_{l=1}^L K_l \sum_{v \in S_l} \{D(W, v) - D_l\}^2 \quad (10)$$

where L isodose levels are selected, S_l represents an isodose surface of the EDDE model, $D(W, v)$ is the dose delivered to a point v from Equation 2, D_l is the normalized dose at the isodose level, and K_l is a weighting factor that determines the relative weight of each isodose in the optimization objective function. In summary, Equation 10 requires that the subarc weighting be selected so that the dose distribution (evaluated on a number of isodoses) predicted by the EDDE model is the one actually being delivered, as estimated by the accurate single beam model. In essence, the EDDE model plays the role of a fast model for determining the optimal subarc configuration, along with isocenter positioning and weighting.

For Equation 10, we usually select the 100% and 60% isodose levels with equal weights in order to keep the dose conformality and sharp dose fall-off outside the target, which is the most important part of the dose distribution. Since the cost function we formulated is a least-square-error problem, we use Singular Value Decomposition⁷ to solve the optimal beam weights vector W , while keeping W_i non-negative.

RESULTS

Experiments for the EDDE model

All the experiments presented in this part were designed to establish our dose model, in which we used a hemispheric phantom as a simple model of the head.^{15,27} We first examined the location, orientation, and size invariance (within a size normalization factor) of EDDE, and then derived the mathematical model from the experiments. For this reason, we constructed a computational head phantom by adjoining a hemisphere with a cylinder and placing an ellipsoidal target at different locations and orientations within this phantom. For each target, we used the methods described in the Methods section. We established that a single formula, namely the one given by Equation 5, describes the dose distribution produced by the EDDE model, independent of the size, position, and orientation of

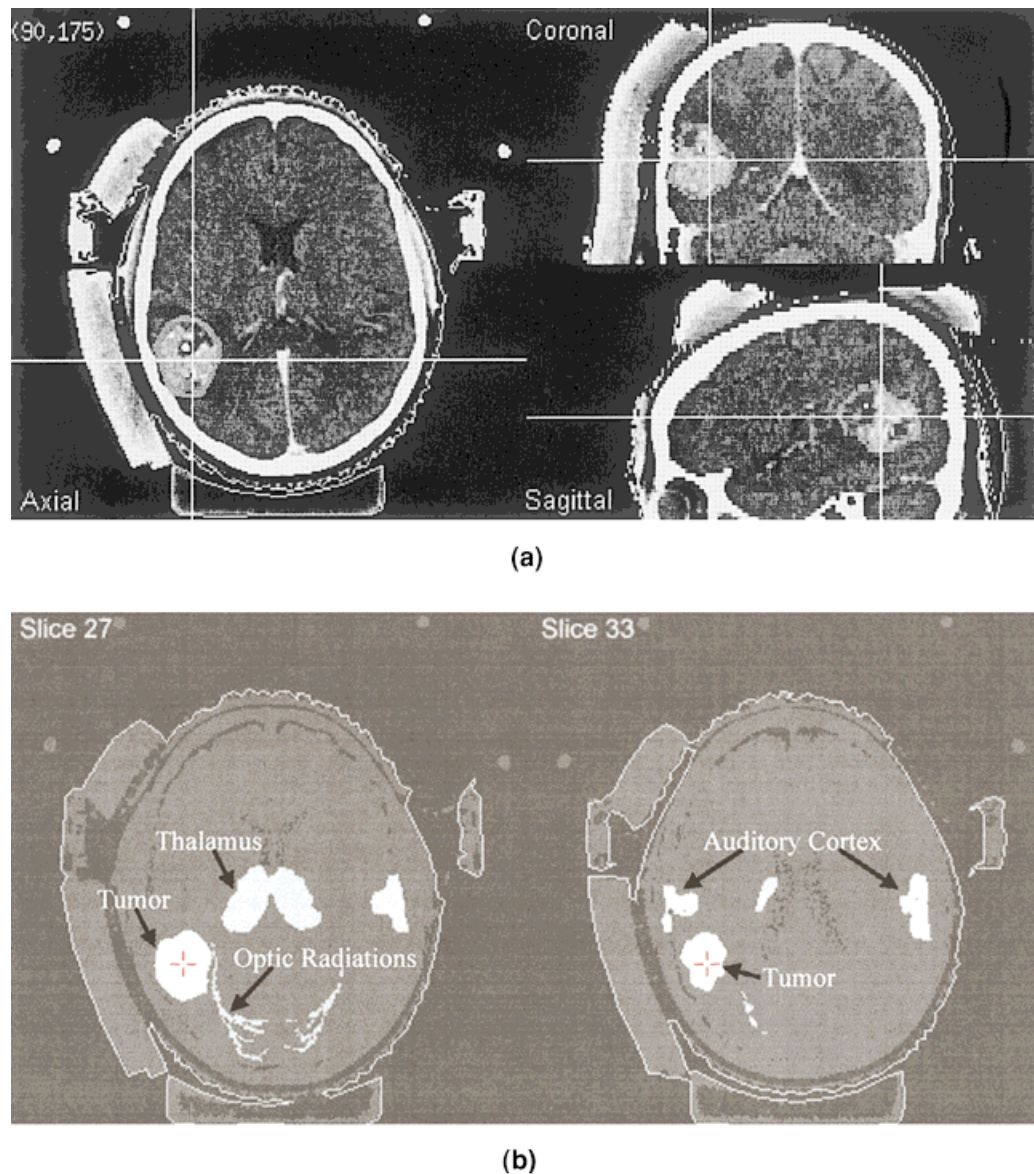


Fig. 5. A clinical case shown in triplanar views. (a) original CT image; (b) segmented image with critical structures labeled. The critical structures were obtained by elastically adapting a digital anatomical atlas.^{30,31}

the target. As an example, Figure 3 shows that the dose distribution produced by the EDDE model, after the appropriate size normalization, follows the same profile for a wide variety of collimator sizes.

Robustness to Local Minima

Since the objective function (Equations 6–9) optimized during the ellipsoid placement is relatively complex and highly non-linear, it is subject to local minima. In order to better understand the behavior of our optimization procedure, we designed experiments to test if the result was sensitive to the initial conditions, and in particular the initial isocenter

placement. We used the clinical case shown in Figure 5. Using the clustering method described in the *Ellipsoid placement* section above, we determined the initial guess of the isocenter positions. We then perturbed the isocenters by displacements ranging from ± 3 mm to ± 10 mm and used the new positions to initialize iterative optimization for the placement of the ellipsoids. For all cases, the resulting optimal ellipsoids were identical, regardless of the initialization. Therefore, we conclude that our algorithm is not sensitive to local minima. This is because we do not optimize individual beams, but rather optimize the placement of larger

components, i.e., ellipsoids, which renders our method more robust to local minima.

Clinical Cases Using the EDDE Model

The case considered herein is shown in Figure 5, which is from a patient with a solitary brain metastasis in the left lateral frontoparietal region.

1. Optimized vs. manual

This was a very large tumor and could not be covered by the largest available collimator size (34 mm), so multiple isocenters were required. This case was used to compare our treatment plan with the plan that was implemented clinically. During the treatment of the patient, the surgeons selected two isocenters and, according to their routine procedures, prescribed 80% isodose (5 Gy) to the tumor volume. In order to achieve the dose conformity to this large irregular target, our surgeons used different collimator sizes for the two isocenters, one with collimator diameters 28 mm and 34 mm, and the other with diameters 18 mm and 21 mm. The arc orientation and beam weighting were adjusted as well. The resulting dose volume histogram (DVH) (Plan Manual) is shown in Figure 6a (dotted line), from which it can be seen that the goal was achieved in terms of target coverage. However, many hot spots inevitably resulted, and the maximum target dose actually went up to 190%. We then re-implemented a treatment plan (Plan Opt1) by using the optimization method presented in this paper. The DVH is shown in Figure 6a as a solid line. While maintaining the same (or even slightly better) target coverage, the EDDE model reduced the hot spots within the target (more than 50% reduction in the 120% to 140% dose range), and the maximum target dose was decreased to 160%. Figure 6b shows the DVH for the normal tissue. The optimized plan delivered a relatively higher dose to normal tissue for lower dose levels. However, it reduced the high dose (higher than 60%) to normal tissue, as compared to the manual plan. Therefore, the optimized plan is superior for achieving both dose homogeneity and conformity.

2. Consideration of critical structures

We next used a deformable registration method⁵ to estimate the location of three critical structures that were displaced by the tumor, using the Talairach atlas of the human brain. To illustrate the behavior of our method, we selected the optic radiations, thalamus, and primary auditory cortex that were close to the tumor (see Figure 5). We assigned high importance factors (δ_h and δ_l in Equation 6) to the

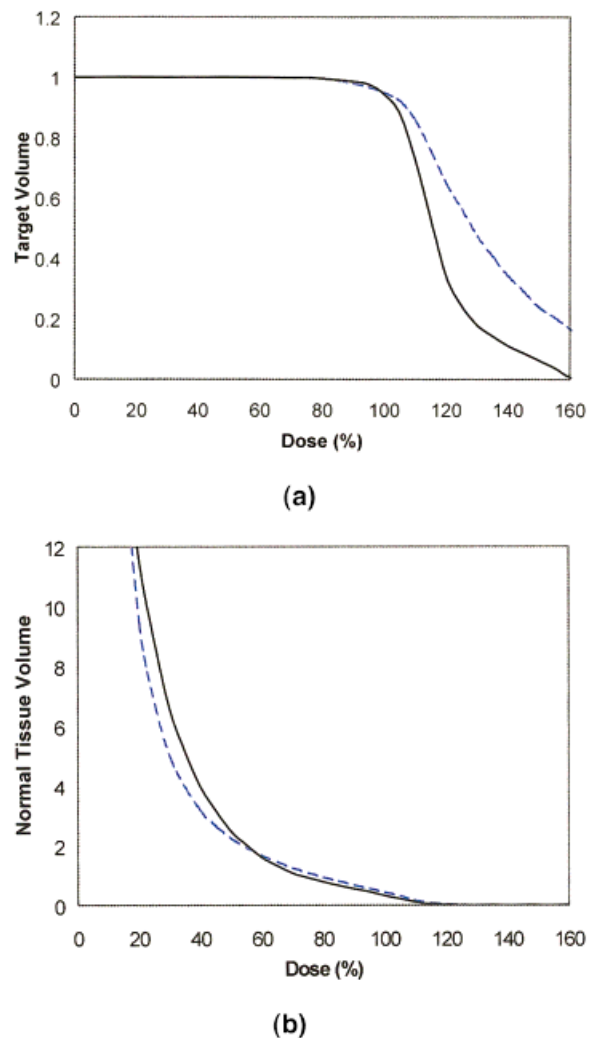


Fig. 6. Dose volume histogram for (a) the target volume, (b) the normal tissue. Dotted lines show the treatment planned manually (Plan Manual). Solid lines show the optimized treatment plan (Plan Opt1). Dose is shown the 100% = 6.25 Gy. Volume is normalized to one for the target volume.

tumor ($\delta_h = 40$ and $\delta_l = 50$) and the three critical structures ($\delta_h = 40$ and $\delta_l = 0$), relative to other normal tissue ($\delta_h = 1$ and $\delta_l = 0$). In addition, the dose tolerance bound (T_h and T_l in Equation 6) was set lower for the avoidance regions ($T_h = 0.1$) relative to that of normal tissue ($T_h = 0.5$). The result is shown as a comparison between the Plan Opt1 described above, which did not differentiate between critical structures and other normal tissue, and the plan implemented here (Plan Opt2), which considered the three critical structures separately.

Obviously, when the critical structures are considered, the target coverage and dose homogeneity would be expected to get worse. Figure 7

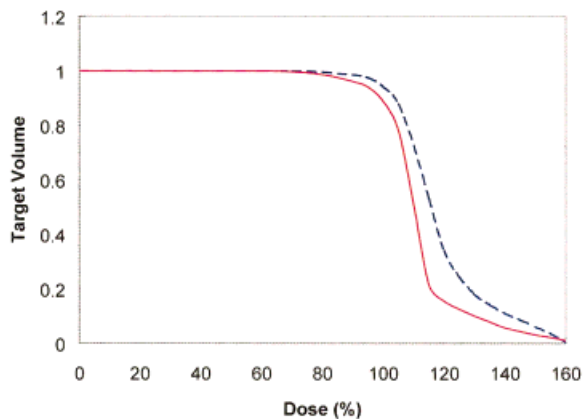


Fig. 7. Dose volume histogram for the target volume. The solid line represents Plan Opt2, in which critical structures were assigned higher importance than the rest of the normal tissue. The dotted line represents Plan Opt1. Volume is normalized to one for the target volume. The prescribed target dose corresponds to the 80% level.

shows the histogram for the tumor, where the solid line corresponds to Plan Opt2 and the dotted line corresponds to Plan Opt1. We observe that, below the 80% dose level, both plans are very similar. Moreover, the tail of the DVH is also the same for both plans. A price was paid in the 80–100% region, but this is minimal, since the prescribed dose was at the 80% level. Therefore, we can say that very little was compromised in terms of tumor coverage by considering the critical structures. Figure 8 shows the histograms for the three critical structures, optic radiations, thalamus, and primary auditory cortex, respectively. We can see that the doses delivered to the thalamus and auditory cortex are clearly reduced, because they are relatively distant from the target. The improvement on the optic radiations is relatively smaller, because the optic radiations are directly adjacent to the target. However, the improvement is concentrated in the high-dose ($> 60\%$) region, in which the dose reduction is very high, percentage-wise. The histograms for the other normal tissues (not shown) were not substantially different between the two plans. Figure 9 shows the resulting isodose contours for the three plans described above, at two different levels in the brain.

In summary, when the importance of the critical structures was raised, our algorithm was able to deliver lower doses to these structures without any serious compromises. Note that, in our system, we do not assume a particular level of importance for each structure, since one cannot do this objectively. Instead, we allow the physician to define these

parameters, while the system finds plans that come as close as possible to the physician's requirements. Because the optimization procedure is relatively fast (2-3 minutes on a Silicon Graphics Workstation), the physician can iteratively modify the importance parameters while evaluating the resulting optimal plans.

3. More complex target shape

In our final experiment, we applied our method to a more complex target and used three isocenters. The resulting DVH is shown in Figure 10, along with several isodose surfaces in axial, coronal, and sagittal sections.

DISCUSSION

We have presented a model-based method for plan optimization in stereotactic radiosurgery using an EDDE model. Several groups^{15,17,22} have also reported methods for producing an ellipsoidal dose distribution. However, there are three major differences between our EDDE model and these other methods. First, we determined analytical forms that

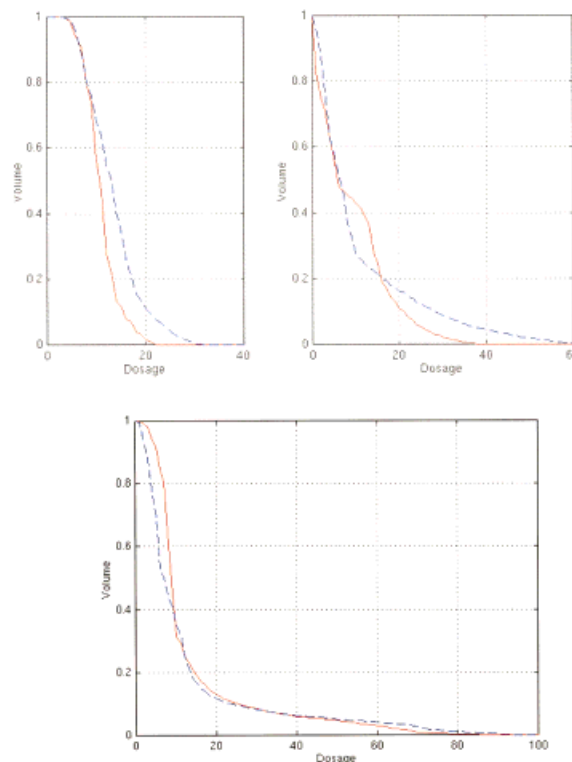


Fig. 8. Dose volume histogram for the thalamus (top left), the primary auditory cortex (top right), and the optic radiations (bottom). The solid line represents Plan Opt2, the dotted line represents Plan Opt1. Volume is normalized to one for each critical structure.

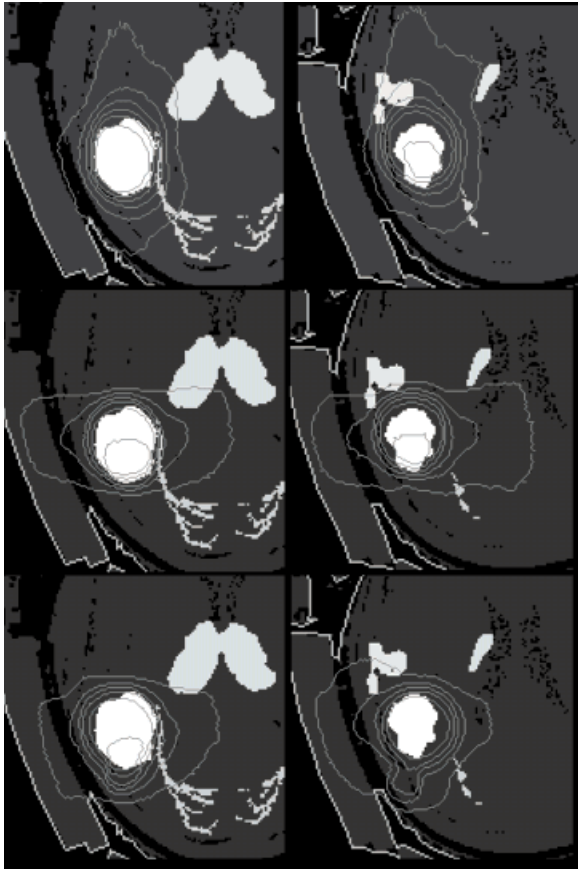


Fig. 9. Isodose contours at two different levels (left and right columns). Top, middle, and bottom rows correspond to the manual plan, Plan Opt1, and Plan Opt2, respectively.

quantitatively describe the dose as a function of distance from the isocenter. Second, only orthogonally placed ellipsoids were investigated by the earlier studies, while our method can produce arbitrarily oriented ellipsoidal dose distributions. Third, the reported ellipsoidal dose distributions are concerned only with the 80% isodose level. In contrast, our technique considers more than one isodose level.

It should be stressed that the parameters of the dose model presented here were determined only for the 10-MeV linac system that we used, and were constrained by the limited availability of collimator sizes. However, the model can be adapted to other systems.

Regarding the optimization methodology that we applied, we note that one could use simulated annealing in order to find the global minimum, as has been previously used successfully in conformal radiation therapy.²⁹ We used Powell's method in our optimization system primarily for its simplicity and computational efficiency, but also because we

demonstrated the robustness of our methodology to local minima. Therefore, random optimization methods are probably not necessary for our approach.

It is important to note that, in our experiments, we imposed many restrictions on our algorithm in order to be able to compare the results with clinically implemented plans on the same cases. This hampered the ability of our planning methodology to obtain more conformal plans. For example, since only circular collimators were available in our clinic, we had to restrict the lengths of the two axes of the reference ellipsoid to being equal. Moreover, we modified Powell's method so that it was restricted by the discrete number of available collimator sizes (13, 16, 18, 21, 28, and 34 mm). Finally, we restricted the beam weight so that it remained constant during the sweep of a subarc. These restrictions would be lifted with a dynamic MMLC system, potentially resulting in considerably more conformal plans. In that case, the EDDE model could, perhaps, be extended to a family of isocenter-based models that are analogous to the ellipsoidal model. If these fundamental "dose components" are represented by relatively few parameters, they could be included in an optimization

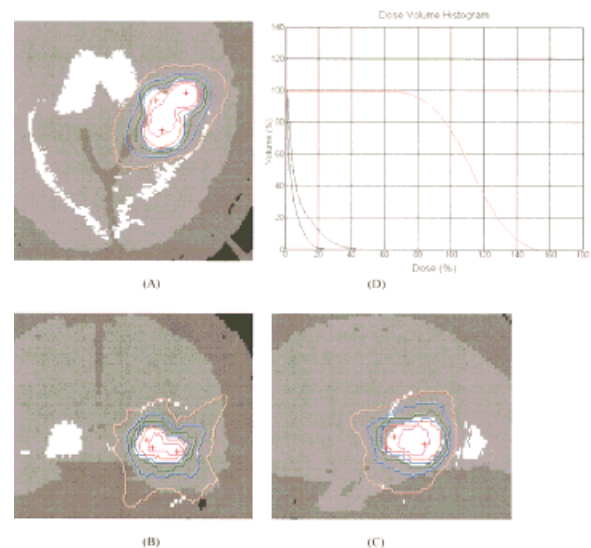


Fig. 10. A case with a rather complex target shape. Shown are isodose images — (A) axial, (B) coronal, (C) sagittal — and (D) a dose volume histogram for thalamus, optic radiations, and tumor (curves from left to right, respectively). Dosage is shown as the percentage of the prescribed dose, volume is shown as the percentage of the volume of the structure itself. Isodose curves are shown from 20 to 120%, with an increment of 20%, from the outermost to the innermost. The isocenters are shown as crosses.

framework similar to the one described here, in which the optimal partitioning of the tumor by a number of such fundamental dose components will result in even better dose conformity. We can expect to achieve a wider variety of shapes for the fundamental components of the dose distribution; this will make our optimal planning more challenging, but more effective in achieving dose conformity. Work towards that end is currently underway in our laboratory.

ACKNOWLEDGMENTS

This work was supported in part by the Center for Computer Integrated Surgical Systems and Technology, funded by the National Science Foundation.

REFERENCES

- Bardash M, Amols HI, Kohn S, Martel MK, Wu CS, Sisti M, Chang CH. Rapid dose calculations for stereotactic radiosurgery. *Med Phys* 1992;19:965–970.
- Bourland JD, Wu QR. Use of shape for automated, optimized 3D radiosurgical treatment planning. *Lecture Notes in Computer Science: Visualization in Biomedical Computing* 1996;1131:553–558.
- Criss TB, Davatzikos C, Liao R, Williams JA. Constrained optimization for stereotactic radiosurgery using deformable neuroanatomical models (Abstract). *Int J Radiat Oncol Biol Phys* 1998;42:361(Suppl).
- Croft MJ. Stereotactic radiosurgery of arteriovenous malformations. *Radiol Technol* 1990;61:375–379.
- Davatzikos C. Spatial normalization of 3D images using deformable models. *J Comput Assist Tomogr* 1996;20:656–665.
- Flickinger JC, Lunsford LD, Wu A, Maitz AH, Kalend AM. Treatment planning for gamma knife radiosurgery with multiple isocenters. *Int J Radiat Oncol Biol Phys* 1990;18:1495–1501.
- Grandjean P, Plantoni K, Lefkopoulos D, Merienne L, Schlienger M. Use of a general inverse technique for the conformational stereotactic treatment of complex intracranial lesions. *Int J Radiat Oncol Biol Phys* 1998;41:69–76.
- Hartmann GH, Schlegel W, Sturm V, Kober B, Pasty O, Lorenz WJ. Cerebral radiation surgery using moving field irradiation at a linear accelerator facility. *Int J Radiat Oncol Biol Phys* 1985;11:1185–1192.
- Kooy HM, Nedzi LA, Loeffler JS, Alexander E III, Cheng CW, Mannarino EG, Holupka EJ, Siddon RL. Treatment planning for stereotactic radiosurgery of intra-cranial lesions. *Int J Radiat Oncol Biol Phys* 1991;21:683–693.
- Kubo HD, Pappas CT, Wilder RB. A comparison of arc-based and static mini-multileaf collimator-based radiosurgery treatment plans. *Radiother Oncol* 1997;45(1):89–93.
- Lam CF, Zhu JG, Fenn JO, Jenrette JM III. Treatment planning optimization for multiple arcs stereotactic radiosurgery using a linear accelerator. *Int J Radiat Oncol Biol Phys* 1995;33:647–657.
- Leavitt DD, Gibbs FA Jr, Heilbrun MP, Moeller JH, Takach GA Jr. Dynamic field shaping to optimize stereotactic radiosurgery. *Int J Radiat Oncol Biol Phys* 1991;21:1247–1255.
- Lu HM, Kooy HM, Leber ZH, Ledoux RJ. Optimized beam planning for linear accelerator-based stereotactic radiosurgery. *Int J Radiat Oncol Biol Phys* 1997;39:1183–1189.
- Lutz W, Winston KR, Maleki N. A system for stereotactic radiosurgery with a linear accelerator. *Int J Radiat Oncol Biol Phys* 1988;14:373–381.
- Luxton G, Jozsef G. Single isocenter treatment planning for homogeneous dose delivery to nonspherical targets in multiarc linear accelerator radiosurgery. *Int J Radiat Oncol Biol Phys* 1995;31:635–643.
- Luxton G, Jozsef G, Astrahan MA. Algorithm for dosimetry of multiarc linear-accelerator stereotactic radiosurgery. *Med Phys* 1991;18:1211–1221.
- Meeks SL, Buatti JM, Bova FJ, Friedman WA, Mendenhall WM. Treatment planning optimization for linear accelerator radiosurgery. *Int J Radiat Oncol Biol Phys* 1998;41:183–197.
- Nedzi LA, Kooy H, Alexander E III, Gelman RS, Loeffler JS. Variables associated with the development of complications from radiosurgery of intracranial tumors. *Int J Radiat Oncol Biol Phys* 1991;21:591–599.
- Nedzi LA, Kooy HM, Alexander E III, Svensson GK, Loeffler JS. Dynamic field shaping for stereotactic radiosurgery: a modeling study. *Int J Radiat Oncol Biol Phys* 1993;25:859–869.
- Olsson LE, Arndt J, Fransson A, Nordell B. Three-dimensional dose mapping from gamma knife treatment using a dosimeter gel and MR-imaging. *Radiother Oncol* 1992;24:82–86.
- Phillips MH, Stelzer KJ, Mayberg MR, Winn HR. Effects of irradiation geometry on treatment plan optimization with linac-based radiosurgery. *Med Phys* 1996;23:1399–1406.
- Plazas MC, Lefkopoulos D, Schlienger M. The influence of arc weights on the dose distribution for single target radiosurgery. *Med Phys* 1993;20:1485–1490.
- Popescu GF, Rodgers JE, von Hanwehr R. Optimization of dose distribution for LINAC based radiosurgery using elliptical collimators. *Acta Neurochir Suppl* 1995;63:35–39.
- Saunders WM, Winston KR, Siddon RL, Svensson GH, Kijewski PK, Rice RK, Hansen JL, Barth NH. Radiosurgery for arteriovenous malformations of the brain using a standard linear accelerator: rationale and technique. *Int J Radiat Oncol Biol Phys* 1988;15:441–447.
- Serago CF, Lewin AA, Houdek PV, Gonzalez-Arias S, Abitbol AA, Marcial-Vega VA, Piscioti V, Schwade JG. Improved linac dose distributions for radiosurgery with elliptically shaped fields. *Int J Radiat Oncol Biol Phys* 1991;21:1321–1325.
- Shiu AS, Kooy HM, Ewton JR, Tung SS, Wong J, Antes K, Maor MH. Comparison of miniature multileaf collimation (MMLC) with circular collimation

- for stereotactic treatment. *Int J Radiat Oncol Biol Phys* 1997;37:679–688.
27. Suh TS, Bova FJ, Yoon SC, Choe BY, Kim MC, Shinn KS, Bahk YW, Ha SW, Park CI. Computer-aided design optimization with the use of a fast dose model for linear-accelerator-based stereotactic radiosurgery. *Phys Med Biol* 1996;41:675–696.
 28. Voges J, Treuer H, Sturm V, Buchner C, Lehrke R, Kocher M, Staar S, Kuchta J, Muller RP. Risk analysis of linear accelerator radiosurgery. *Int J Radiat Oncol Biol Phys* 1996;36:1055–1063.
 29. Webb S. Optimization by simulated annealing of three-dimensional conformal treatment planning for radiation fields defined by a multileaf collimator. *Phys Med Biol* 1991;36:1201–1226.
 30. Weeks KJ, Marks L, Ray SK, Spencer DP, Turner DA, Friedman AH. 3-dimensional optimization of multiple arcs for stereotactic radiosurgery. *Int J Radiat Oncol Biol Phys* 1993;26:147–154.
 31. Williams J, Enger C, Wharam M, Tsai D, Brem H. Stereotactic radiosurgery for brain metastases: comparison of lung carcinoma vs. non-lung tumors. *J Neurooncol* 1998;37:79–85.
 32. Winston KR, Lutz W. Linear accelerator as a neurosurgical tool for stereotactic radiosurgery. *Neurosurgery* 1988;22:454–464.
 33. Yan Y, Shu H, Bao X, Luo L, Bai Y. Clinical treatment planning optimization by Powell's method for gamma unit treatment system. *Int J Radiat Oncol Biol Phys* 1997;39:247–254.